Title
CARS Temperature Measurements in a Droplet Stream Flame

Journal
Combustion Science and Technology, 83(1-3)

ISSN
0010-2202

Authors
ZHU, JY
DUNN-RANKIN, D
SAMUELSEN, GS

Publication Date
1992-05-01

DOI
10.1080/00102209208951825

Combust. Sci. and Tech., 1992, Vol. 83, pp. 97–114
Photocopying permitted by license only

CARS Temperature Measurements in a Droplet Stream Flame

J. Y. ZHU, D. DUNN-RANKIN and G. S. SAMUELSEN *Department of Mechanical and Aerospace Engineering, University of California, Irvine, California 92717*

(*Received January 7, 1991; in final form July 30, 1991*)

Abstract—This paper describes measurments of the local temperature field near a combusting stream of methanol droplets using coherent anti-Stokes Raman scattering (CARS). Synchronizing the CARS measurements with the droplets in the stream allows correlations between the temperature field and the droplet position. These measurements describe the thermal structure of the droplet stream flame and can help validate detailed spray combustion models. The diameter of the droplets in the stream is 120 μm, which is comparable to the droplet size in a practical spray. The droplet spacing is approximately 1.0 mm (8 droplet diameters). The CARS measurements indicate a flame surrounding the droplet stream located 1 mm (8 droplet diameters) from the stream centerline. The temperature profile shows a local minimum temperature a the stream centerline. Moving radially outward from the centerline, the temperature rises at the flame (about 2000 K), and then falls gradually to room temperature. The local minimum temperature is more pronounced on lines through droplet centers than on lines between adjacent droplets. The results also show that the temperature profile between adjacent droplets becomes more uniform as the droplets move downstream.

Key words: CARS, temperature, droplets, flame

INTRODUCTION

Experimental studies of the combustion of a single droplet, a droplet array, or a droplet stream are valuable because these combustion processes can duplicate essential features of realistic spray flames while avoiding the complex behavior of the spatial and temporal distributions of droplet size and velocity present in full sprays. In addition, some basic spray combustion models have been developed for combusting droplet streams (Rangel and Sirignano, 1988, 1989) and combusting droplet arrays (Chiang and Sirignano, 1990) where experimental verification can be useful.

The applicability to spray flames of previous single droplet and droplet stream combustion experiments is limited by larger droplet sizes than the size found in practical sprays (*e.g.*, $\approx$ 1 mm in Miyasaka and Law, 1981; $\approx$ 1 mm in Xiong *et al.*, 1984; $\approx$ 2 mm in Brzustowski *et al.*, 1979; $\approx$ 1–4 mm in Brzustowski *et al.*, 1981), and by experimental methods that preclude the measurement of temperature and concentration (Sangiovanni and Kesten, 1976; Sangiovanni and Dodge, 1978; Twardus and Brzustowski, 1978; Koshland and Bowman, 1984; Quieroz and Yao, 1989). Recently, Montgomery *et al.* (1990) reported temperature and concentration measurements in a multiple droplet stream flame. However, they measured the temperature field with a thermocouple so they could not obtain the local temperature field near individual droplets.

Measuring the thermal field in a droplet stream flame is difficult because liquid droplets affect most common temperature probes, and because the combustion regime has very steep gradients over a small spatial scale. Fortunately, coherent anti-Stokes Raman scattering (CARS) has the capability for spatially resolved, non-intrusive temperature measurements in droplet and particle laden flows (Eckbreth and Hall, 1979; Beiting, 1985; Dunn-Rankin *et al.*, 1990). The coherent nature of the CARS signal ensures strong discrimination from the background, even with droplets or particles in the flow.

CARS is a nonlinear four optical wave mixing process that can be used to interrogate the energy state of an ensemble of molecules. The use of CARS as a diagnostic tool has developed with the availability of high power lasers. In the spatially resolved (or BOXCARS) configuration, the CARS signal is generated by the interation of three incident laser beams (two pumping beams and one Stokes beam) within the CARS probe volume through the third order nonlinear susceptibility of the medium under investigation. When the frequency difference between the pumping beam and the Stokes beam coincides with the frequency of a Raman-active mode of the medium (normally a vibrational-rotational transition), the CARS signal is resonantly enhanced. From quantum mechanics, the CARS energy spectrum is a predictable function of the medium temperature. Therefore, the temperature can be determined by comparing the experimental CARS spectrum to a spectrum calculated using temperature as a fitting parameter. Complete reviews of the CARS process (Druet and Taran, 1981; Valentini, 1985) and a discussion of CARS as a combustion diagnostic (Eckbreth, 1988) are available in the literature.

This paper demonstrates the capabilities of CARS to measure temperature near combusting droplets, and presents measurements of the temperature field near droplets in a droplet stream flame. The goal of the present work is to correlate the temperature field with the droplet position in a combusting droplet stream, and thereby provide the temperature field surrounding a burning droplet and the behavior of this field as the droplet moves downstream. The results from these experiments provide insight into the structure and behavior of spray flames, and can validate detailed numerical models (*e.g.*, Delplanque and Rangel, 1991).

EXPERIMENTAL APPARATUS

The experimental apparatus uses a monodisperse droplet generator and hydrogen ignition source to generate a droplet stream flame. Temperature measurements utilize a mobile CARS system in the BOXCARS configuration, and a frequency divider circuit synchronizes the CARS measurements with the droplet generation process. In addition, a schlieren system, using the CARS laser as a synchronized light source, provides qualitative images of the droplet stream and flame. Further details of the experimental apparatus appear in the following subsections.

CARS System

The CARS system is set up on a two level optical cart, and the optical layout on the cart is shown in Figure 1. The 1064 nm laser beam from a 10 Hz injection seeded Nd:YAG laser (Spectra-Physics DCR-3) is frequency doubled through SHG1 to provide a primary 532 nm laser beam. The primary 532 nm laser beam splits at the 30/70 beamsplitter BS1. The 30% leg pumps the dye laser amplifier DC2. The 50/50 beamsplitter BS4 splits the 70% leg into the two pumping beams of the BOXCARS. The residual 1064 nm radiation from the first frequency doubler passes the harmonic separator HS1 and is doubled by SHG2 to provide a secondary 532 nm laser beam. The secondary beam pumps the dye laser oscillator DC1. We use a 0.55×10^{-4} molar mixture of Rhodamine 640 dye (Exciton) in methanol for both the oscillator and the amplifier stages of the dye laser. This mixture produces a broadband Stokes beam centered at 607 nm for the BOXCARS system. The transmitting optics include mirrors, a prism delay loop (P3, P4), telescope lenses to collimate the laser beams (L3, L4, L5, L6), and the 250 mm focal length projection lens (L7). The projection lens

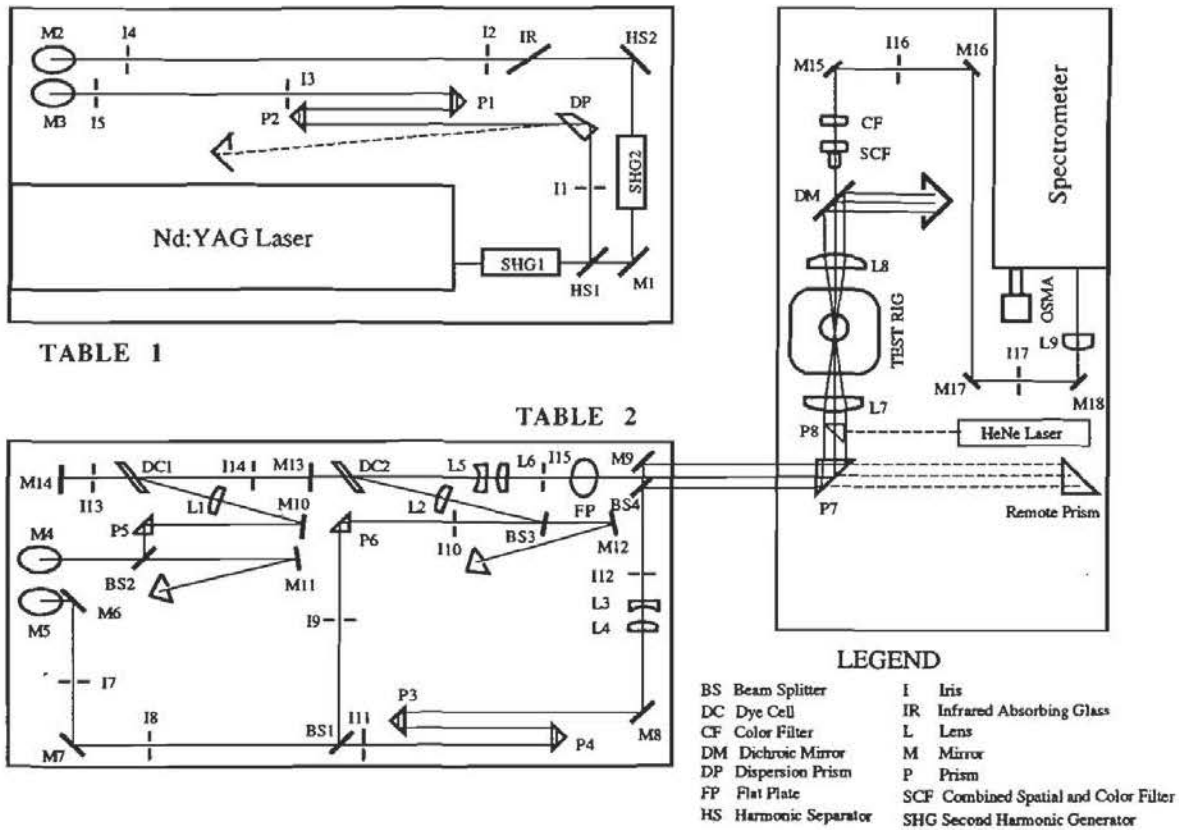

FIGURE 1 Schematic of the experimental CARS system. Table 1 is below Table 2 on a moveable cart. Mirrors M2, M3, M4, and M5 represent periscopes to bring laser light from Table 1 to Table 2.

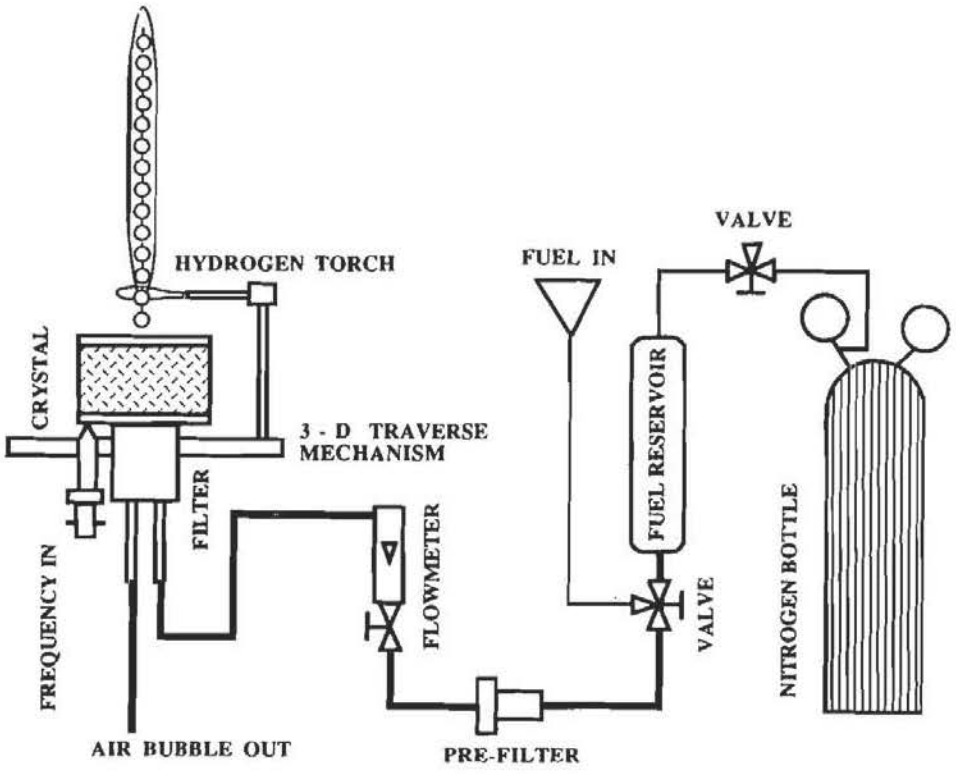

FIGURE 2 Schematic of the droplet generator and droplet stream flame.

focuses the two 532 nm pumping beams and the dye laser beam to a probe volume in the center of the droplet stream flame. The beam crossing angle is 3°. A second 250 mm focal length lens (L8) collects the CARS signal and passes it through filters to a spectrometer (SPEX 1702/04). An intensified diode array (Princeton Instruments IRY—1024 IPDA) records the CARS spectrum at the exit of the spectrometer.

Droplet Stream Flame

A vibrating orifice droplet generator, similar to the one described by Berglund and Liu (1973), generates a steady monodisperse droplet stream. A hydrogen diffusion flame at the tip of a 27 gauge needle ignites and pilots the droplet stream flame. Both the droplet generator and the hydrogen flame reside on a three dimensional traverse mechanism which allows a full spatial mapping of the temperature field. The distance between the droplet generator and the hydrogen flame remains unchanged during the traverse, maintaining constant boundary and initial conditions for the combusting droplet stream. A schematic of the droplet generator is shown in Figure 2. Pressurized nitrogen drives the liquid fuel out of the reservoir and through a 50 μm diameter orifice. The orifice vibrates with the piezoelectric crystal driven by square waves from a function generator. At particular frequencies, the crystal vibration breaks up the fuel jet issuing from the orifice into a monodisperse droplet stream. For these experiments, we use a nitrogen pressure of 20 psig, methanol liquid, and a vibration

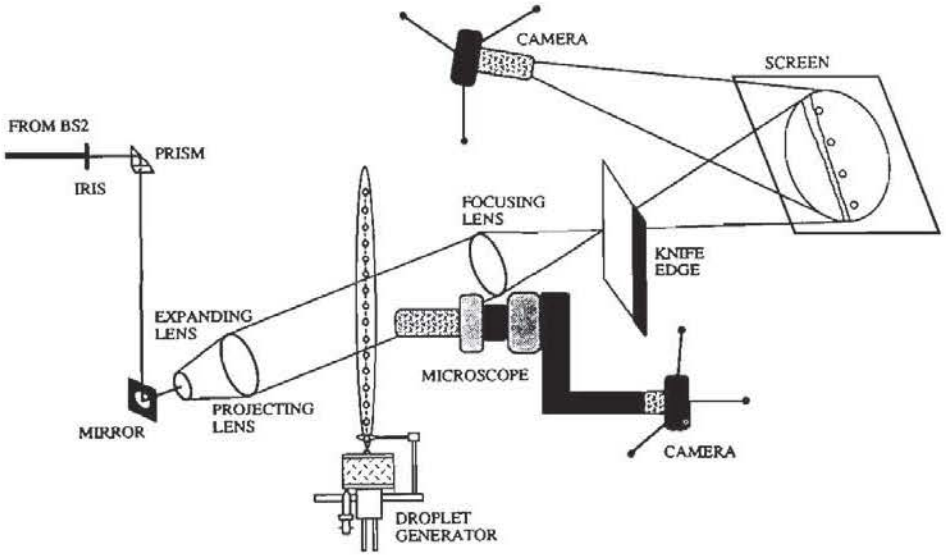

FIGURE 3 Schematic of the schlieren system.

frequency of 9.8 kHz. Under these operating conditions, the droplet generator produces droplets of approximately 120 μm diameter, with droplet-to-droplet spacing of 1.0 mm. Droplets traverse the measurement zone with a velocity of approximately 10 m/s.

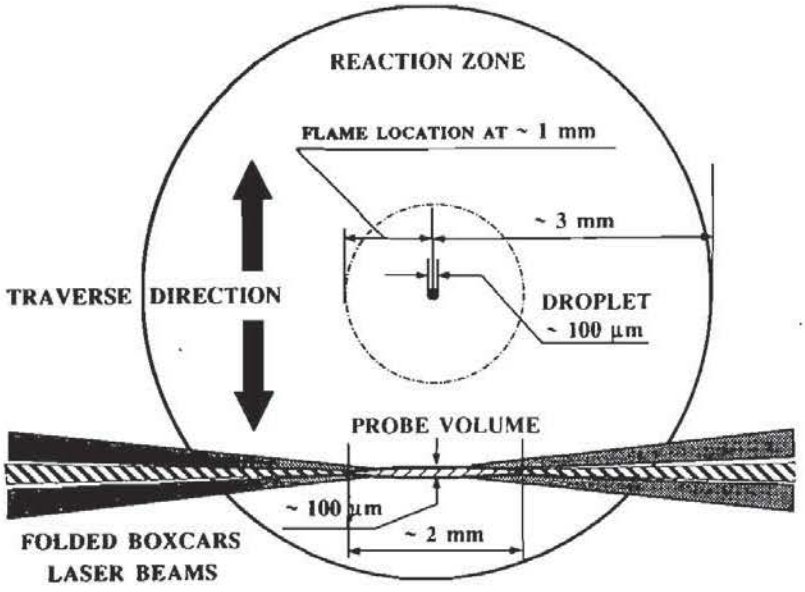

FIGURE 4 Size of CARS probe volume relative to droplet and droplet stream flame.

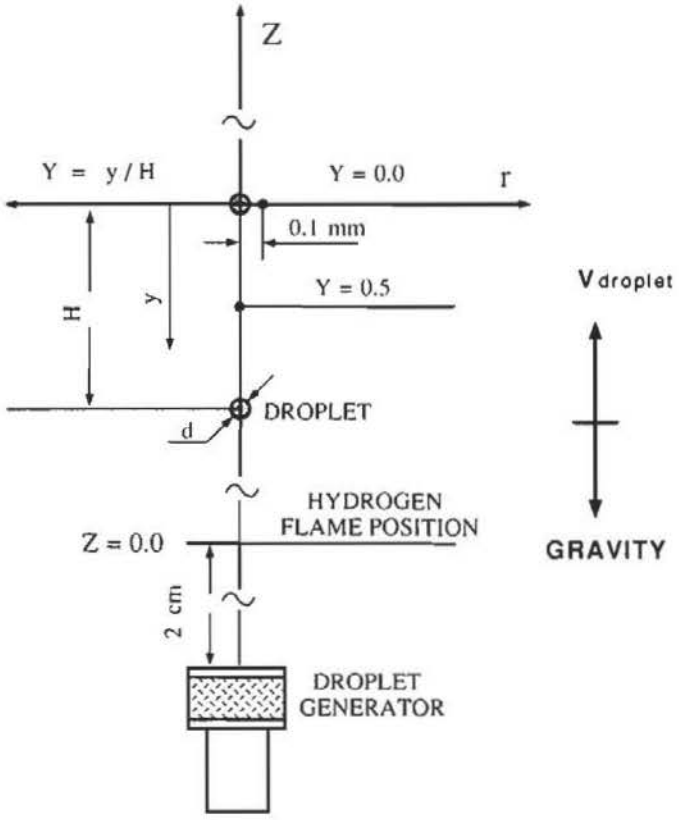

FIGURE 5 Schematic showing the measurement locations and the nondimensional spatial variables used to present the results.

Electronics

A frequency dividing circuit synchronizes the YAG laser firing with the droplet generator. The synchronization ensures that the CARS probe volume remains in the same position relative to the droplets for each sequence of measurements. The synchronous measurement allows the correlation of the droplet position with the temperature field. A function generator sends 20 V peak-to-peak square waves to the piezoelectric crystal to vibrate the drop generator orifice. The TTL output of the function generator is input to the 12 bit frequency divider, and the output from the divider triggers the Nd:YAG flashlamps. In our experiments, the divider drives the laser at 9.6 Hz, which is close to the 10 Hz design operating frequency of the laser. The laser can run between 8.5–11.5 Hz without significant power loss.

Schlieren System

Figure 3 shows how the schlieren system employs the Nd:YAG laser as light source. As shown in the figure, the laser light comes from BS2 after M11 is removed. Because the laser beam has a "doughnut" intensity profile, an iris picks off a 1 mm diameter uniform intensity spot from the expanded beam. A prism and mirror direct the light from this spot through a beam expanding lens (25 mm focal length, 25 mm diameter). An achromat collimating lens (350 mm focal length, 63 mm diameter) projects the

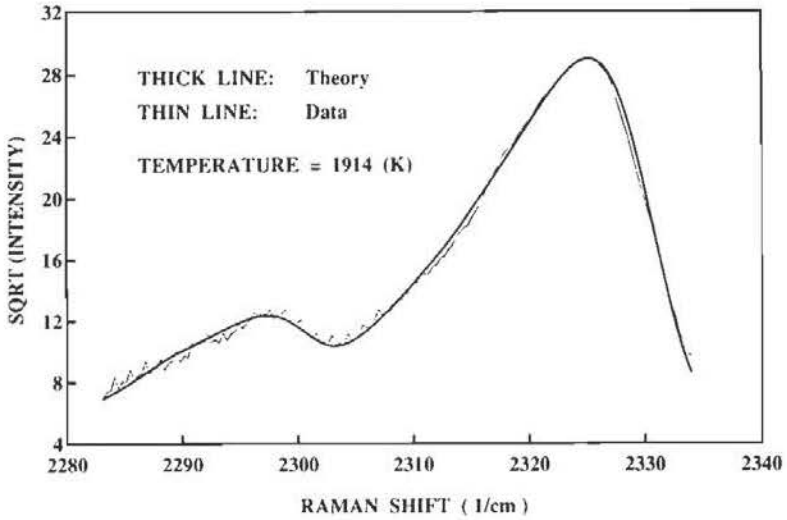

FIGURE 6 Typical comparison between measured and calculated CARS spectra in the high temperature region of the droplet stream flame.

light across the droplet stream flame. Another achromat collects the light and focuses it past the knife edge and onto a screen. A 35 mm camera (Canon T-70) with a 70–200 mm zoom lens transfers the screen image to 100 ASA color slide film. Satisfactory photographs required 1 second exposures, corresponding to approximately 10 laser shots. The clarity of the droplet images over this exposure time indicate an extremely stable droplet stream.

Experiment Resolution

From visual observation, the droplet stream flame is only about 2 mm thick. To effectively map the temperature field of such small dimension requires high spatial resolution. The droplets act as edge markers for measuring the diameter of the probe volume. After measuring the size of the droplets photographically, we translate the CARS probe volume across the droplets while recording the region producing an audible and visible laser induced breakdown. The total traverse distance where breakdown occurs less the droplet diameter is twice the CARS probe diameter. Using this method, the CARS probe volume is $100 \pm 15\,\mu$m. The length of the CARS probe volume is measured by observing the resonant CARS signal while translating a stack of glass slides through the beam overlap region. The extreme points where the resonant signal appears and disappears marks the extent of the CARS probe volume. Using this method, our probe volume is approximately 2 mm long, with most of the signal generated in the central 1.5 mm region.

Figure 4 shows the relative sizes and locations of the CARS probe volume, the droplet, and the flame. To obtain accurate temperature measurements, we traverse the droplet generator perpendicular to the long axis of the CARS probe volume as indicated in Figure 4. Between the droplet surface and the reaction zone (< 1 mm from the droplet) the CARS probe volume is large relative to the spatial dimensions of the region. Near the droplet, therefore, the temperature measurements represent a spatially averaged temperature. Because CARS is a non-linear process, however, the

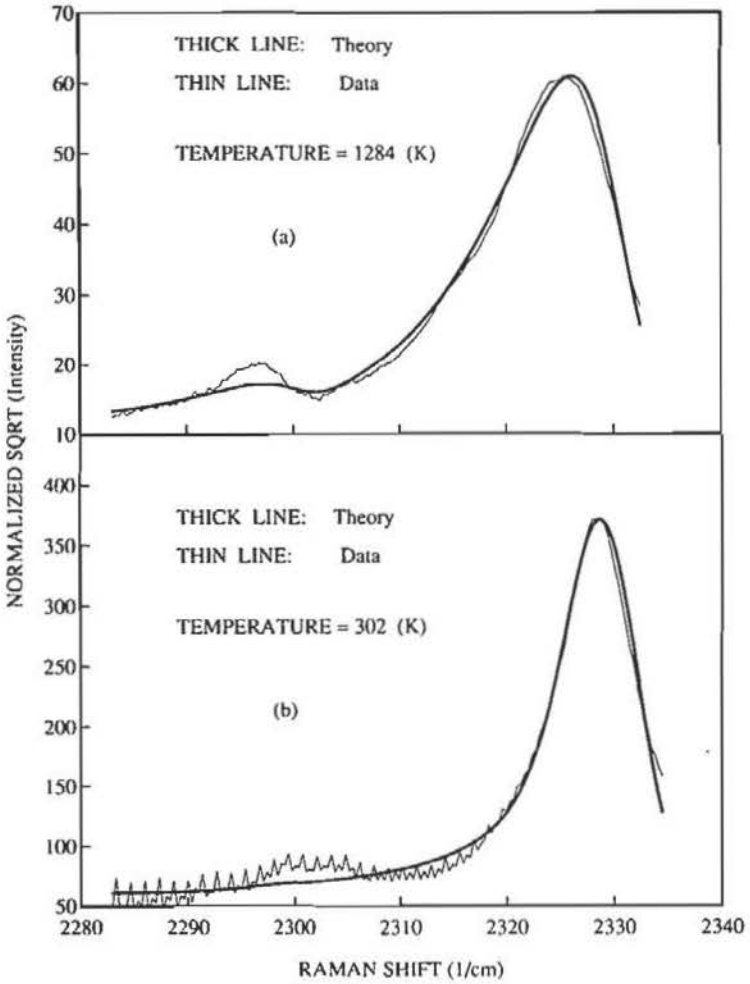

FIGURE 7 Typical comparison between measured and calculated CARS spectra in the (a) moderate and (b) low temperature regions of the droplet stream flame.

spatial average is not simply a density weighted average. Instead, a sum of contributions from the third-order susceptibility at different temperatures produce a single composite CARS spectrum. This composite spectrum is then fit to a single temperature. Calculations using the Sandia CARS Code indicate that for a 2 mm CARS probe length the spatial averaging smooths out sharp temperature peaks near the flame and produces significant temperature errors only very near the droplet (< 2 diameters). The spatial averaging effects diminish with increasing distance from the droplets and are negligible at radial distances larger than 15 drop diameters. Similar effects of CARS spatial averaging in a turbulent flame sheet have been reported by Shepherd *et al.* (1990).

The droplets in the stream flame move downstream at 10–15 m/s. The Nd:YAG laser pulse, however, is only 15 ns. Consequently, the droplets are effectively motionless during each CARS temperature measurement. Multiple exposure (500 laser shots) backlit droplet images indicate that, relative to the CARS measurement volume, the

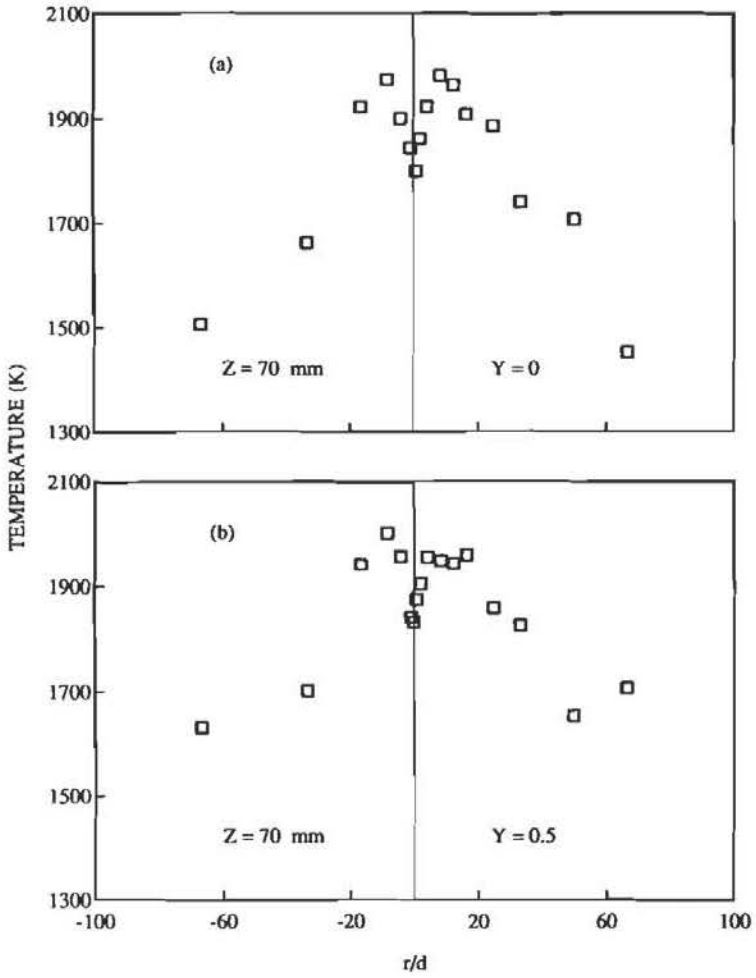

FIGURE 8 CARS temperature measurements across the droplet stream flame 70 mm downstream of the ignition source. (a) the on-droplet profile $Y = 0.0$; (b) the between-droplet profile $Y = 0.5$.

droplet position fluctuates less than 100 μm in the axial direction and less than 20 μm perpendicular to the droplet stream.

EXPERIMENT SUMMARY

The experimental conditions for the results reported in this paper are: methanol fuel, a 50 μm diameter orifice in the droplet generator, a liquid fuel of 20 psig, a hydrogen flow rate of 15 cc/min to the ignition pilot flame, and a droplet generator vibration frequency of 9.8 kHz. These conditions produced 120 μm diameter droplets spaced 1.0 mm apart. We measure the droplet size and spacing with a microscope and reticle. The droplet spacing measurement is verified by focusing the CARS beams onto one droplet, and then recording the vertical traverse necessary to focus the beams onto the adjacent droplet. The digital divide circuit fired the YAG laser at 9.6 Hz. The measurement location nearest the orifice is 70 mm downstream of the hydrogen flame.

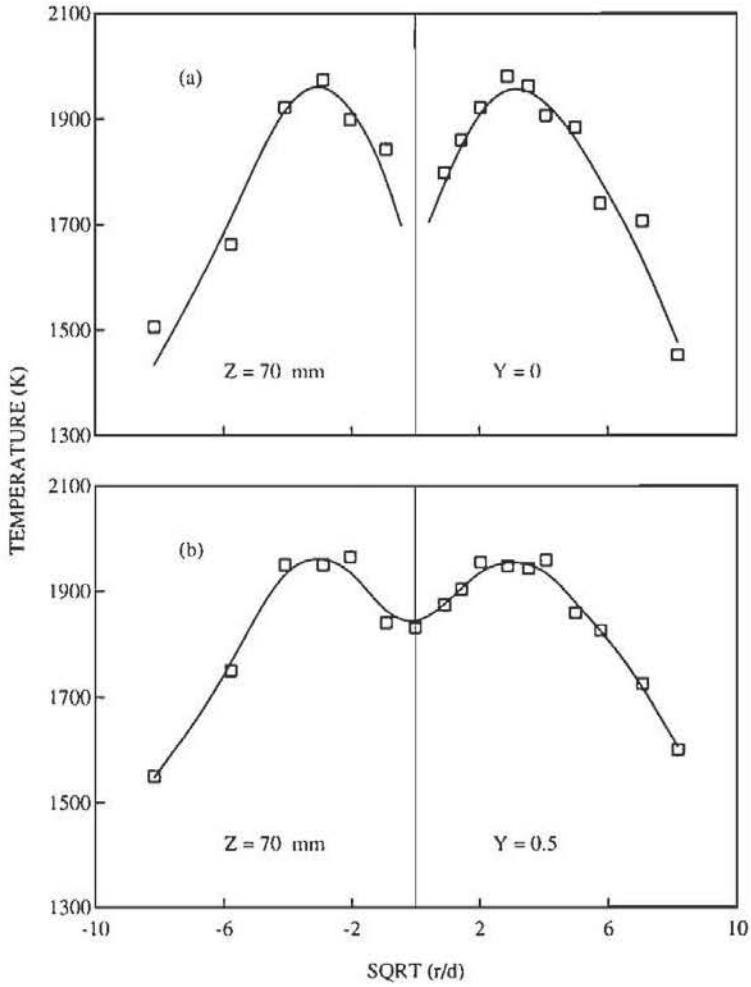

FIGURE 9 The same measurements as shown in Figure 8, but now temperature is plotted versus $\sqrt{r/d}$ to expand the near droplet region. The solid lines are smooth splines fit to the data. (a) the on-droplet profile $Y = 0.0$; (b) the between-droplet profile $Y = 0.5$.

Thermocouple measurements indicate that at this distance the hydrogen flame does not have significant effects on the droplet flame temperature. The results include 4 radial temperature profiles. Figure 5 shows the geometric relation between the droplet stream flame and these measurement locations, where r is the radial coordinate from the droplet center outward. The nondimensional coordinate Y measures distance along the droplet stream axis, and is the distance from the droplet center divided by the droplet spacing ($Y = y/H$). For $Y = 0$, corresponding to the plane of the droplet center, measurements begin 100 μm from the droplet center to avoid laser induced droplet breakdown. There are 16 points in each temperature profile. To improve the signal-to-noise ratio, each CARS measurement represents an average of 5 laser shots, and each data point is an average of 100 measurements.

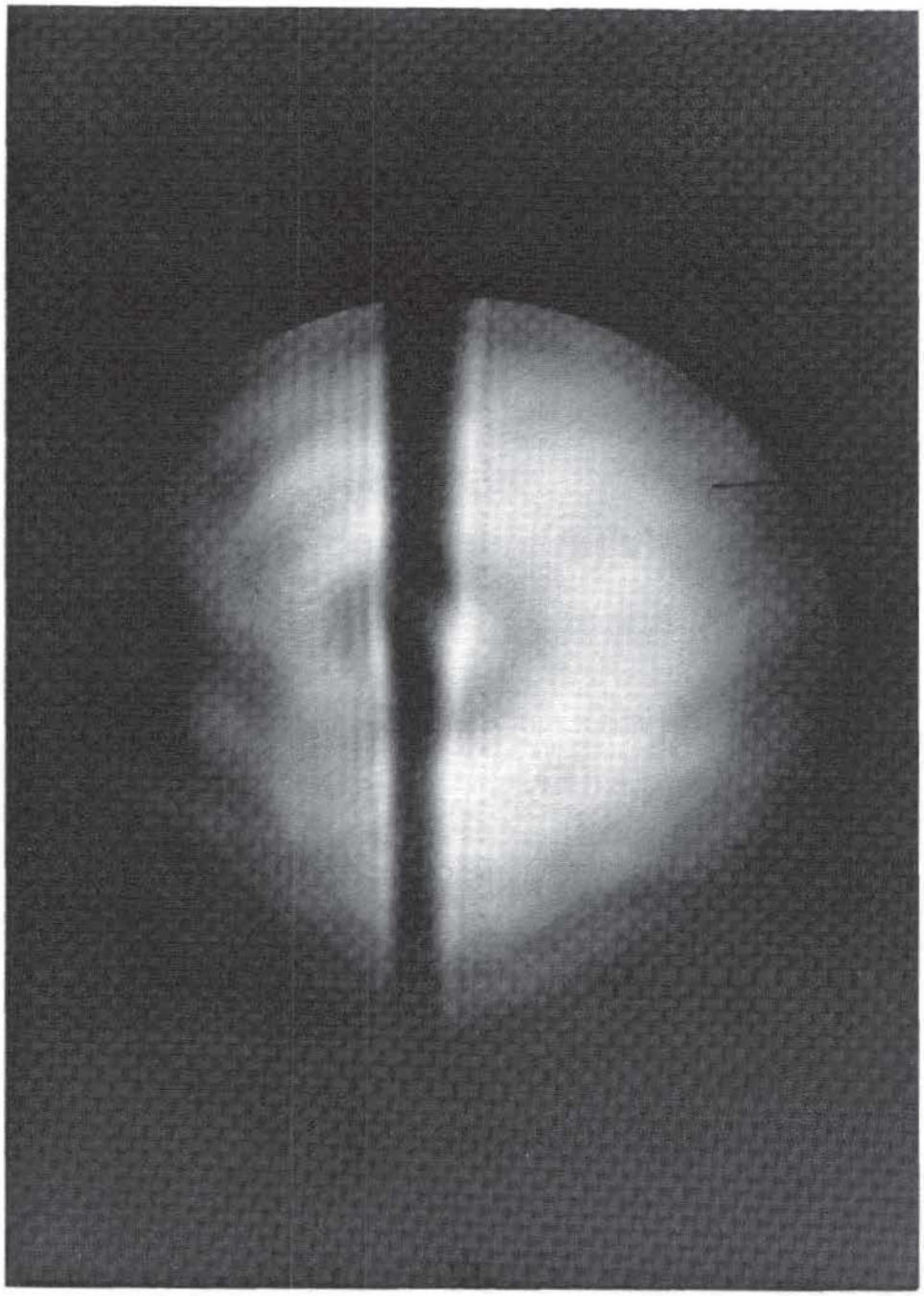

FIGURE 10 Schlieren photograph of the droplet stream flame. The photograph includes 10 iluminating laser shots over a 1 s exposure time. The upper dark line indicates $Z = 100$ mm and the lower dark line indicates $Z = 70$ mm.

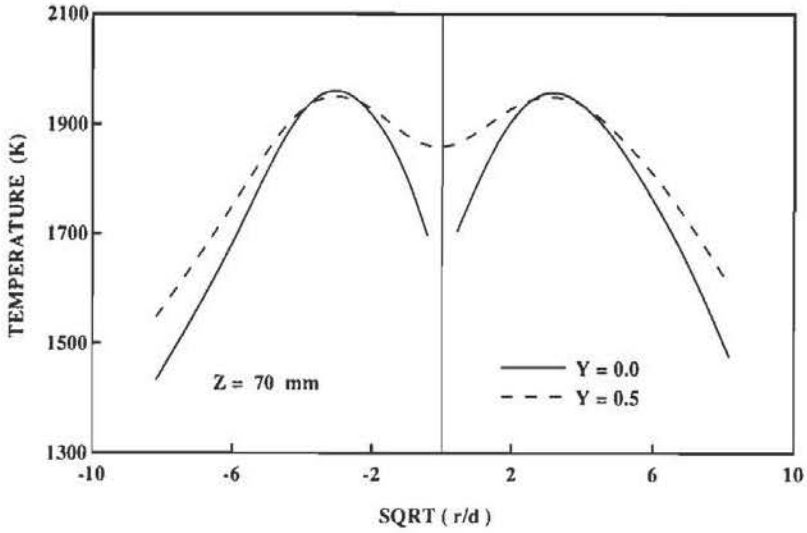

FIGURE 11 Comparison of the on-droplet and between-droplet temperature profiles 70 mm from the ignition source.

RESULTS AND DISCUSSION

Spectrum Fitting

To extract temperature from CARS measurements requires a spectral fitting procedure that matches experimental CARS spectra to theoretical CARS spectra using temperature as a fitting parameter. Our fitting procedure employs a library of theoretical nitrogen CARS spectra over the range from 250–3000 K in 50 K increments. The Sandia CARS code CARSFT (Palmer, 1989) generates the spectral library by assuming an instrument function deduced from the fit to a room temperature nitrogen CARS spectrum measured in the CARS system. The CARSFT code has been extensively used and validated with CARS measurements in combustion systems (*e.g.*, Farrow *et al.*, 1984; Lucht *et al.*, 1987; Boyack, 1990). Preparing the experimental CARS spectra for fitting requires a background subtraction, normalization by the dye laser profile, and taking the square root of the result. A modified version of the Sandia quick fitting code FTCARS (Palmer, 1990) finds the temperature whose associated theoretical spectrum mostly closely matches the experimental spectrum. The quick fitting program linearly interpolates between temperatures represented in the spectral library to find the least squares best fit between measured and calculated spectra. Rejecting spectra with poor signal-to-noise ratio coupled with visual checks of the fit for several spectra at each measurement location helps ensure reliable experimental results. With this procedure, the absolute temperature error is less than 100 K, and the standard error of the temperature at each measurement location is less than 25 K.

The methanol concentration varies significantly from the droplet surface to the flame front. Because hydrocarbons have large non-resonant susceptibility (Farrow, *et al.*, 1987), this variation can affect the CARS temperature fit. The fit can be improved by allowing the nonresonant susceptibility to vary as a fitting parameter (Hall and Boedeker, 1984). In measurements near the droplet surface, where the methanol concentration is high, variation in the nonresonant susceptibility from the

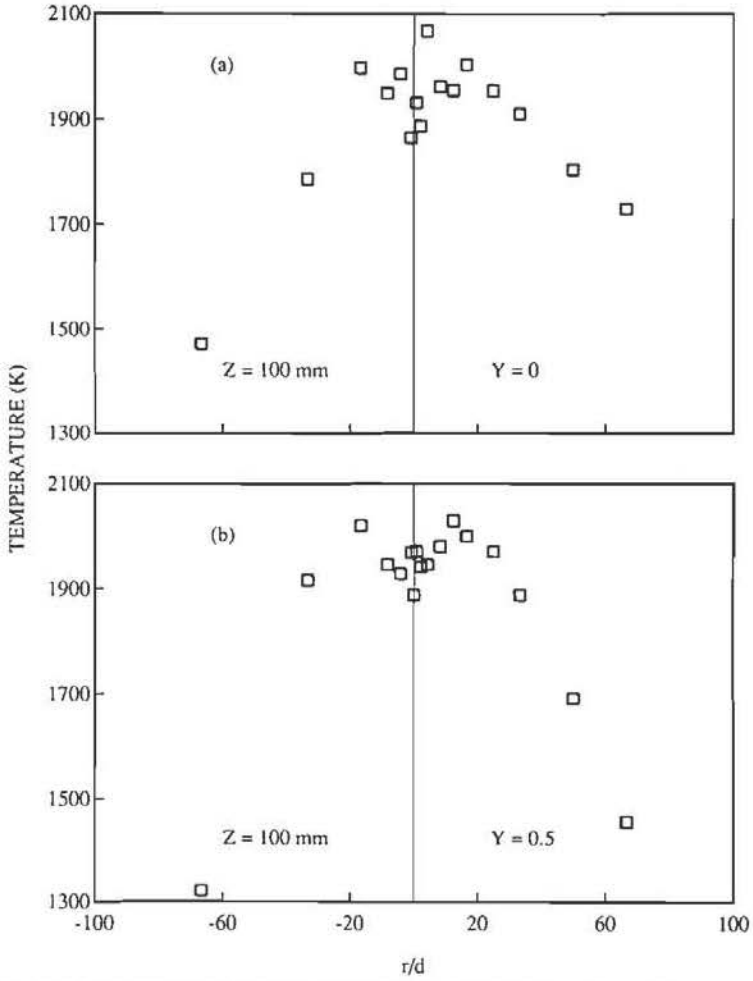

FIGURE 12 CARS temperature measurements across the droplet stream flame 100 mm downstream of the ignition source. (a) the on-droplet profile $Y = 0.0$; (b) the between-droplet profile $Y = 0.5$.

value of nitrogen to the best fit value changes the predicted temperature by less than 75 K.

Figure 6 shows a typical spectral fit for measurements less than 9 mm from the stream centerline. The small scale random fluctuations come from noise in the detector. While the fit is very good, the first hot band is slightly more pronounced in the measured spectrum than in the calculated spectrum, and the fundamental band is slightly narrower in the measurement than in the calculation. This vibrationally hot and rotationally cool behavior was noted by Snelling *et al.* (1989), who ascribed the phenomenon to stimulated Raman pumping to the vibrationally excited $v = 1$ level. In their analysis, Snelling *et al.* found that stimulated Raman pumping affected high temperature spectra by less than 50 K. However, to ensure that stimulated Raman pumping does not affect the droplet stream flame CARS measurements, we take a series of spectra at a single point in the flame while varying the laser power. The temperature fits to these spectra differ by less than 50 K, indicating that stimulated Raman pumping does not affect high temperature measurements significantly.

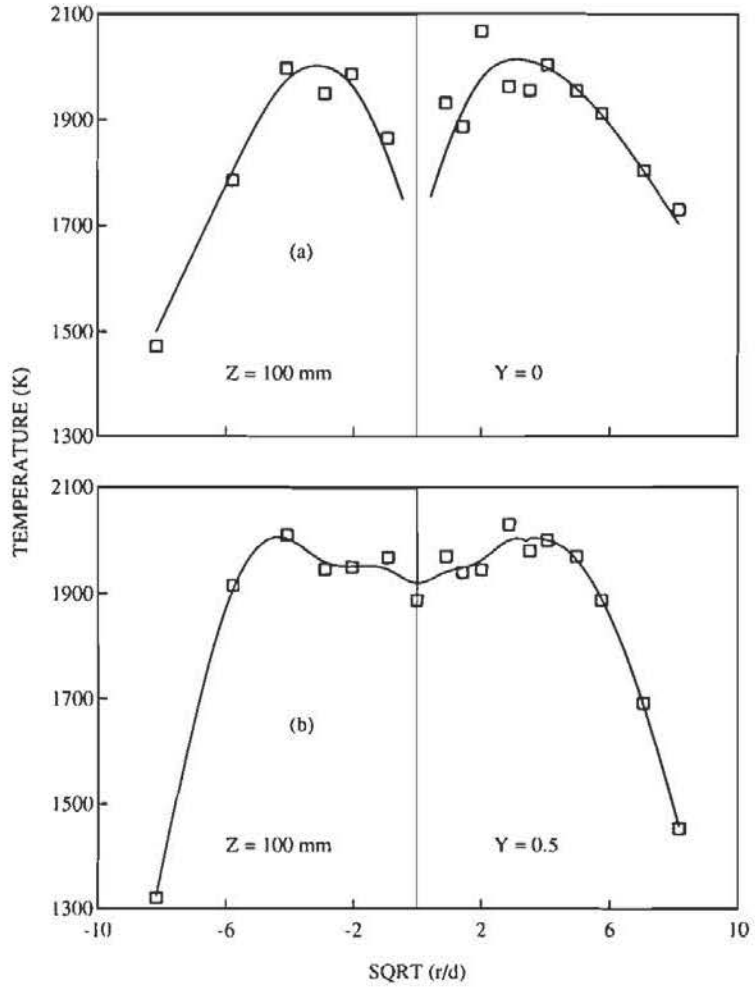

FIGURE 13 The same measurements as shown in Figure 12, but now temperature is plotted versus $\sqrt{r/d}$ to expand the near droplet region. The solid lines are smooth splines fit to the data. (a) the on-droplet profile $Y = 0.0$; (b) the between-droplet profile $Y = 0.5$.

For measurements far from the droplet, where the temperature is less than 1400 K, the stimulated Raman pumping is more pronounced, making accurate analysis of the cool spectra difficult. Figure 7 shows two examples of cool spectra with significant stimulated Raman pumping. While it is possible to fit only the fundamental band of these spectra to get the temperature, such fits can be unreliable, particularly for temperatures above 800 K. Consequently, this paper does not report measurements in the cooler regions of the flame. Reduced laser power coupled with improved signal collection in future experiments should help reduce the stimulated Raman pumping effect.

Local Temperature Field Characteristics

Figure 8 shows two temperature profiles 70 mm downstream of the hydrogen flame ignition source. Figure 8(a) shows the radial temperature profile at the droplet

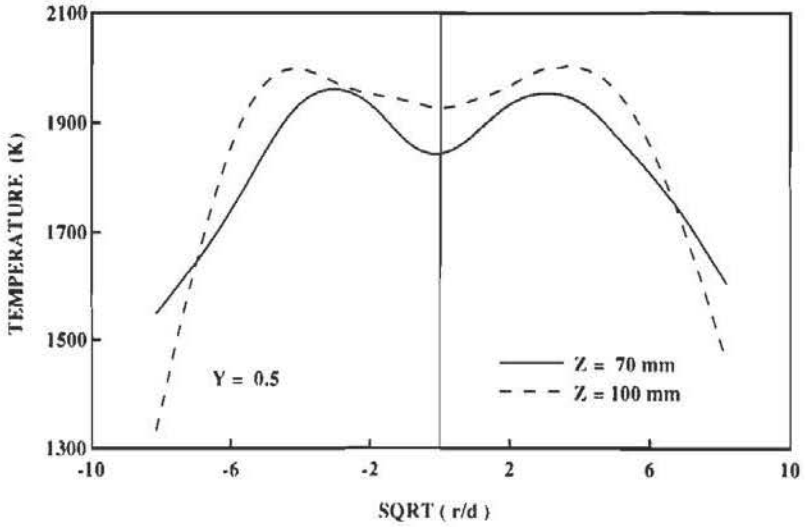

FIGURE 14 Comparison between the between-droplet temperature profiles 70 mm and 100 mm downstream of the ignition source.

centerline ($Y = 0$), and Figure 8(b) shows the profile between two droplets ($Y = 0.5$). Figure 8 plots temperature versus the nondimensional distance r/d, where d is the droplet diameter. Because the flame zone is small relative to the extent of the flame's thermal influence, it is useful to expand the near-droplet region using $\sqrt{r/d}$ on the abscissa. Figure 9 shows the expanded temperature profiles, with Figure 9(a) giving the $Y = 0$ profile, and Figure 9(b) showing the $Y = 0.5$ profile. The solid lines in the figures are smooth spline fits to the data. Because the droplet is present, the $Y = 0$ results include data only to within 100 μm of the droplet stream axis. Including data on both sides of the droplet centerline helps describe the symmetry of the flame.

Figures 8 and 9 show a temperature maximum of 2000 K at $r/d = 10$ for both the $Y = 0$ and $Y = 0.5$ cases. This maximum is 10% below the 2200 K adiabatic flame temperature of methanol/air flames. The on-droplet $Y = 0$ case shows a more rapid increase in temperature from the stream axis to the maximum than does the between-droplet $Y = 0.5$ case. The difference results from the presence of a droplet at $Y = 0$. The temperature decrease on the axis for the $Y = 0.5$ case suggests that the droplets are not surrounded by individual spherical flames, but burn collectively. For radial positions outside the temperature maximum, the temperature profiles for $Y = 0$ and $Y = 0.5$ are similar, suggesting a nearly cylindrical flame sheet around the droplet stream. The schlieren photograph of the droplet stream flame in Figure 10 also indicates a cylindrical flame sheet. The photograph is a 10 laser shot exposure. The two dark lines indicate CARS measurement locations, with the top line at $Z = 100$ mm and the bottom line at $Z = 70$ mm. The image shows a dark flame edge only to the side of the droplet stream, not between droplets, indicating collective combustion. In similar experiments with larger droplets, Twardus and Brzustowski (1978) also concluded that their droplet stream burned collectively, and not as individual droplets.

It is interesting that the $Y = 0$ case in Figure 8 indicates that the temperature profile is concave down between the droplet surface and the flame. This qualitative

shape agrees with the classical description of individual droplet combustion in Glassman (1987) and with detailed computations of droplet combustion by Rangel and Fernandez-Pello (1984).

Figure 11 compares the shape of the temperature profiles at $Y = 0$ and $Y = 0.5$ by overlaying the smooth splines from Figures 9(a) and 9(b). The comparison shows that the maximum flame temperature is nearly the same for the on-droplet and between-droplet cases. The between-droplet profile is broader and more uniform, but the location of the maximum temperature coincides with the maximum of the on-droplet profile. This result suggests that at the 70 mm location the flame stand-off distance from the centerline does not depend on the location of the droplet.

Figures 12 and 13 are similar to Figures 8 and 9, except that the measurements are taken 100 mm downstream of the ignition source. At this location, the scatter in the data is higher, and the overall temperatures are slightly higher than at the 70 mm location, but the shape of the profiles at the two locations are similar. Figure 14 compares the $Y = 0.5$ profiles between the 70 mm and 100 mm measurement location. The downstream profile has slightly higher temperature, a more uniform shape, and a maximum temperature farther from the droplet stream axis. These results suggest that the flame broadens as it progresses downstream. The schlieren photograph of Figure 10 also indicates a slight broadening of the flame. The increase in temperature, and the more uniform, broader temperature profile, probably results from combustion heat release convected downstream.

SUMMARY

This paper describes a synchronous CARS apparatus for measuring the temperature profile in a droplet stream flame. Using this apparatus we report temperature profile measurements in a droplet stream flame along lines perpendicular to the direction of the droplet travel. Profiles passing through the droplet position, and halfway between adjacent droplets are included. The principal findings of these experiments are:

- Temperatures in the between-droplet profile reveal a local minimum temperature at the droplet stream axis. This minimum, and qualitative schlieren photographs, suggest that the droplets burn collectively, rather than as individual droplets.
- The on-droplet profiles show a steeply rising temperature from near the droplet surface to a maximum temperature at the flame sheet, followed by a temperature decrease to room temperature.
- As the droplets move downstream, the flame temperature increases slightly and the temperature profile becomes broader and more uniform. The data scatter is higher in the downstream measurements suggesting unsteady behavior of the droplet stream flame.

Further work requires improved performance of the CARS system and synchronization system to reduce the fluctuations in the droplet stream that limit the spatial resolution of the measurements. With these improvements, it will be possible to measure the temperature profile between drops along the stream axis, and to reveal further the thermal structure of the droplet stream flame.

ACKNOWLEDGEMENTS

This research is sponsored by the Air Force Environics Laboratory (Contract F08635-90-6-0100) and a Presidential Young Investigator award from the National Science Foundation to one of the authors (DDR) with complementary funding from the Allison Gas Turbine Division of General Motors.

REFERENCES

Beiting, E. J. (1985). Coherent interference in multiplex CARS measurements: nonresonant susceptibility enhancement due to laser breakdown. *Appl. Opt.* **24,** 3010–3017.

Berglund, R. N. and Liu, B. Y. H. (1973). Generation of a monodisperse aerosol standard. *Environmental Sci. Tech.* **7,** 147–153.

Boyack, K. W. (1990). A study of turbulent nonpremixed jet flame of CO/N_2 using coherent anti-Stokes Raman spectroscopy. Ph.D Dissertation, Department of Chemical Engineering, Brigham Young University.

Brzustowski, T. A., Sobiesiak, A., and Wojcicki, S. (1981). Flame propagation along an array of liquid fuel droplets at zero gravity. *18th Sym. (Int.) on Combust.* The Combustion Institute, Pittsburgh,PA, 265–273.

Brzustowski, T. A., Twardus, E. M., Wojcicki, S., and Sobiesiak, A. (1979). Interaction of two burning fuel droplets of arbitrary size. *AIAA J.* **17,** 1234–1242.

Chiang, C. H. and Sirignano, W. A. (1990). Numerical analysis of interacting, vaporizing, fuel droplets with variable properties. 28th Aerospace Science Meeting Paper AIAA-90-0357, Reno, NV, January 8–11.

Delplanque, J-P. and Rangel, R. H. (1991). Droplet-stream combustion in the steady boundary layer near a wall. *Combust. Sci. Tech.* **78,** 97–115.

Druet, S. A. J. and Taran, J. P. E. (1981). CARS spectroscopy. *Prog. Quant. Electr.* **7,** 1–72.

Dunn-Rankin, D., Switzer, G. L., Obringer, C. A., and Jackson, T. A. (1990). Effect of droplet-induced breakdown on CARS temperature measurements. *Appl. Opt.* **29,** 21, 3150–3159.

Eckbreth, A. C. (1988). *Laser Diagnostics for Combustion Temperature and Species*, Abacus Press, Cambridge, MA.

Eckbreth, A. C. and Hall, R. J. (1979). CARS thermometry in a sooting flame. *Combust. and Flame* **36,** 87–98.

Farrow, R. L., Lucht, R. P., and Rahn, L. A. (1987). Measurements of the nonresonant third-order susceptibilities of gases using coherent anti-Stokes Raman spectroscopy. *J. Opt. Soc. Am. B* **4,** 8, 1241–1246.

Farrow, R. L., Lucht, R. P., Flower, W. L., and Palmer, R. E. (1984). Coherent anti-Stokes Raman spectroscopic measurements of temperature and acetylene spectra in a sooting diffusion flame. *20th Sym. (Int.) on Combust.*, The Combustion Institute, Pittsburgh, PA, 1307–1312.

Glassman, I. (1987). *Combustion*, Academic Press, New York, NY, 256.

Hall, R. J. and Boedeker, L. R. (1984). CARS thermometry in fuel-rich combustion zones. *Appl. Opt.* **23,** 1340–1346.

Koshland, C. P. and Bowman, C. T. (1984). Combustion of monodisperse droplet clouds in a reactive environment. *20th Sym. (Int.) on Combust.* The Combustion Institute, Pittsburgh, PA, 1799–1807.

Lucht, R. P., Teets, R. E., Green, R. M., and Ferguson, C. R. (1987). Unburned gas temperatures in an internal combustion engine, I, CARS temperature measurements. *Combust. Sci. Tech.* **55,** 41–61.

Miyasaka, K. and Law, C. K. (1981). Combustion of strongly-interacting linear droplet arrays. *18th Sym. (Int.) on Combust.* The Combustion Institute, Pittsburgh, PA, 283–292.

Montgomery, C. J., Son, S. F., and Queiroz, M. (1990). Temperature and concentration measurements in a turbulent spray flame. Submitted for publication.

Palmer, R. E. (1989). The CARSFT computer code for calculating coherent anti-Stokes Raman spectra: User and programmer information. Sandia National Laboratory Technical Report, SAND 89-8206.

Palmer, R. E. (1990). Private communication, Sandia National Laboratories, Livermore, CA.

Queiroz, M. and Yao, S-C. (1989). A parametric exploration of the dynamic behavior of flame propagation in planar sprays. *Combust. Flame* **76,** 351–368.

Rangel, R. H. and Fernandez-Pello, A. C. (1984). Mixed convective droplet combustion with internal circulation. *Comb. Sci. Tech.* **42,** 47–65.

Rangel, R. H. and Sirignano, W. A. (1988). Two-dimensional modelling of flame propagation on fuel stream arrangements. *Dynamics of Reactive Systems Part II: Heterogeneous Combustion Applications*, Progress in Astronautics and Aeronautics Vol. 13, Kuhl, *et al.*, eds., AIAA, Washington D.C.

Rangel, R. H. and Sirignano, W. A. (1989). Combustion of parallel fuel droplet streams. *Combust. Flame* **75,** 241–254.

Regnier, P. R., Moya, F., and Taran, J. P. E. (1974). Gas concentration measurements by coherent Raman anti-Stokes scattering. *AIAA J.* **12,** 826–831.

Sangiovanni, J. J. and Dodge, L. G. (1978). Observations of flame structure in the combustion of monodispersed droplet streams. *17th Sym. (Int.) on Combust.* The Combustion Institute, Pittsburgh, PA, 455–465.

Sangiovanni, J. J. and Kesten, A. S. (1976). Effects of droplet interaction in ignition in monodispersed droplet streams. *16th Sym. (Int.) on Combust.* The Combustion Institute, Pittsburgh, PA, 577–592.

Shepherd, I. G., Porter, F. M., and Greenhalgh, D. A. (1990). Spatial resolution effects on CARS in turbulent premixed combustion thermometry. *Comb. and Flame* **82,** 106–109.

Snelling, D. R., Smallwood, G. J., and Parameswaran, T. (1989). Effect of detector nonlinearity and image persistence on CARS derived temperatures. *Applied Opt.* **28**, 3233–3241.

Twardus, E. M. and Brzustowski, T. A. (1978). An experimental study of flame speed and burning in arrays of monosize hydrocarbon droplets. *Combust. Sci. Tech.* **17**, 215–225.

Valentini, J. J. (1985). Coherent anti-Stokes Raman spectroscopy. In *Spectrometric Techniques, IV*, Academic Press, New York, NY, 1–59.

Xiong, T. Y., Law, C. K., and Miyasaka, K. (1984). Interactive vaporization and combustion of binary systems. *20th Sym. (Int.) on Combust.* The Combustion Institute, 1781–1787.